The Comparative Study between Back to Back and the Matrix Structure for the Wind Turbine Based on DFIG

Abdelkarim Chemidi[*‡], Sidi Mohammed Meliani[*], Mohamed Choukri Benhabib[*]

[*]Department of Electrical and Electronic Engineering, Faculty of Technology, University of Tlemcen, Algeria

[‡] Corresponding Author; Abdelkarim Chemidi, Tel: +213 554 03 96 49, chemidi.abdelakrim@gmail.com

Received: 13.04.2015 Accepted:24.05.2015

Abstract- This study analyses the performance between back to back and the matrix converters used through wind power system based on double fed induction generator (DFIG). The aim of this comparison is to design which converter is well exploiting wind power generation. It is defined as a comparison for each topology in controls, current quality generated by the DFIG and power losses in converters, every part is given in details with its simulation result. These last show that the better performances are obtained when DFIG is fed by the matrix converter.

Keywords- Wind turbine; Matrix converter; Back to back converter; Power losses; double fed induction generator (DFIG).

1. Introduction

Nowadays, the interest of renewables energies for power creation becomes increasingly useful due to declining of fossil energies more they don't create pollution and effective life. Amongst these energies there is that of the wind which contributes towards power generation.

Recently, the use of wind turbine increases because of improving the power electronics technologies and decreasing of the equipment costs. Wind turbine system consists of a mechanical part as well as an electrical part. The mechanical part includes blades and the gearbox however; the electrical part includes the generator speed and converters. This last one continues to progress.

Overall, many solutions are presented to produce wind power. From the beginning, researchers have been interested on the synchronous machines as generators [1]. For economic reasons, the use of these kinds of generators is becoming more and more down in favor of asynchronous generators. Even a large number of the wind turbine installed in the world focus on the asynchronous, this last has a small range of speed variation that is why people are more interested nowadays on the double fed induction generator (DFIG) for its wide speed variation range. The DFIG is an asynchronous machine consisting of a stator as well as a rotor. Usually, in wind power applications the stator is directly connected to the network whereas; the rotor is connected through the converter to the network. In literature, many configurations are proposed concerning the DFIG. The configuration with back to back converter which is widely discussed [2,3,4] due to its particular advantage which is the bi-directionality of power flow transfer.

Recently, some researchers have studied the DFIG in wind turbines by using the matrix converter to connect the rotor to the grid [5,6,7]. Many strategies are adopted to control the matrix converter. After the initial appearance of matrix converter in 1976, several control algorithms have been proposed such as Venturini [6] and space vector modulation [8]. In this paper, an algorithm called Ph D [9] is used. The advantage of this algorithm rather than the others, it is the simplicity of control and there is no need to a phased locked loop (PLL).

This work includes a comparison between DFIG wind power system using back to back converter and the matrix converter; the aim is to design which one is more performing on wind power application. In this study, 2 essential aspects in wind power generation are discussed; the first one studies the electrical quality (harmonics). The second one consists of power losses comparison between the 2 topologies to know which one is more efficient in the wind turbines.

The wind turbine represents the common part in both topologies so we will firstly present as an overview its model. Then the modeling of the DFIG is presented. After that we will explain in more details each topology with its

own control and simulation results. Finally, the power losses are calculated and the obtained results are presented.

2. Wind Turbine

2.1. Modelling of wind turbine

The wind is the main element to operate wind turbine system. So, the rotation of blades creates a mechanical power P_t on the shaft of the turbine, expressed by [10]:

$$P_t = 0.5\, C_p(\lambda,\beta)\rho\, s\, v^3 \quad (1)$$

where ρ the air density in kg/m^3, s the turbine rotor area in m^2, v the wind speed in m/s, C_p is the power coefficient expressed by [11]:

$$C_p = C_1(C_2(A-B)C_3\beta - C_4)\exp(-C_5(A-B)) + C_6\,\lambda \quad (2)$$

where $A = \frac{1}{\lambda + 0.08\beta^3}$, $B = \frac{0.0035}{\beta+1}$, C_1=0.5109, C_2 = 116, C_3= 0.4, C_4=5, C_5=21, C_6= 0.0068.

λ represents the ratio between the speed at the blade tip and wind speed, β is the blade angle.

The power P_t generates a torque on the shaft (turbine side) given by the following equation [7]:

$$T_t = 0.5\rho C_p\,(\lambda,\beta)\, S\, v^3 \frac{1}{\Omega_t} \quad (3)$$

The speeds (rotor side and turbine side) are joined by the gearbox then the total inertia is as follow:

$$J = \frac{J_t}{G^2} + J_m \quad (4)$$

Finally, the dynamic fundamental equation of the mechanical system on the shaft of the DFIG is given [7]:

$$T_m = J\frac{d\Omega_{mec}}{dt} + f_v\,\Omega_{mec} + T_e \quad (5)$$

2.2. Maximum Power Extraction

The concept is to optimize the generator speed relative to the wind velocity intercepted by the wind turbine such that the power is maximized [11]. However, there are three areas of operation for a variable speed wind turbine, which are:

Area 1: the wind speed is low; consequently the wind turbine can't start.

Area 2: the wind reaches a minimum speed allowing the wind turbine to starts; the shaft speed is adjusted through the electromagnetic torque. A Maximum power point tracking (MPPT) is then necessary.

Area 3: the wind speed is over the rated speed, it implies a risk of damage to the turbine blades, so the pitch control method is used to regulate the turbine speed.

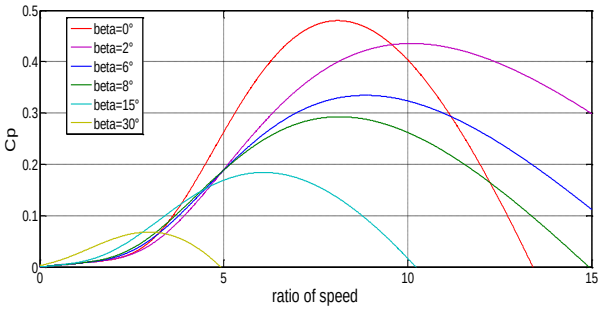

Fig. 1. Power coefficient versus ratio of speed λ and pitch angle β

In area 2 the objective is to extract the maximum power of the turbine. For that the power coefficient should be maximized (C_{p_max} = 0.47). This value is obtained when we have λ_{opt}=8.1; β=0° (see Fig.1)

3. Modelling of the Asynchronous Generator

The schematic representation of the double fed induction generator is shown on Fig.2, where the stator and rotor phases are indicated respectively by (a,b,c) and (A,B,C); the electrical angle θ defines the relative position between the instantaneous axis of the stator and rotor magnetic phase.

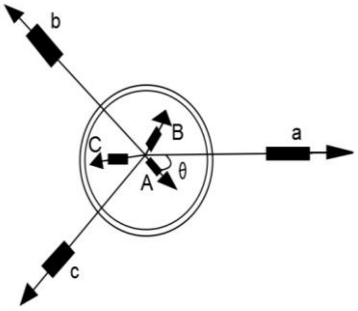

Fig. 2. Schematic representation of DFIG

The matrixes formed by voltages equations of the stator and the rotor are given below [12]:

$$[V_{abc}] = R_s[i_{abc}] + \frac{d}{dt}[\varphi_{abc}] \quad (6)$$

$$[V_{ABC}] = R_r[i_{ABC}] + \frac{d}{dt}[\varphi_{ABC}] \quad (7)$$

where: $[V_{abc}] = [V_a \quad V_b \quad V_c]^T$, $[\varphi_{abc}] = [\varphi_a \quad \varphi_b \quad \varphi_c]^T$, $[i_{abc}] = [i_a \quad i_b \quad i_c]^T$.

Same for the rotor vectors with index changes $[V_{ABC}]\,[\varphi_{ABC}]\,[i_{ABC}]$.

The total flux coupled with phases of stator and rotor is expressed by:

$$[\varphi_{abc}] = [L_s][i_{abc}] + [L_{sr}][i_{ABC}] \quad (8)$$

$$[\varphi_{ABC}] = [L_r][i_{ABC}] + [L_{rs}][i_{abc}] \quad (9)$$

Where $[L_s]$, $[L_r]$ are the matrix of the stator and rotor inductance respectively. $[L_{sr}]$ is the matrix of the mutual inductance stator-rotor. $[L_{rs}]$ is the matrix of the mutual inductance rotor-stator.

By substituting Eq. (8), Eq. (9) in Eq. (6), and Eq. (7) we obtain:

$$[V_{abc}] = R_s [i_{abc}] + [L_s] \frac{d}{dt}[i_{abc}] + \frac{d}{dt}\{[L_{sr}][i_{ABC}]\} \quad (10)$$

$$[V_{ABC}] = R_r [i_{ABC}] + [L_r] \frac{d}{dt}[i_{ABC}] + \frac{d}{dt}\{[L_{rs}][i_{abc}]\} \quad (11)$$

with: $[L_{sr}] = [L_{rs}]^T$

The voltage and flux equations of the DFIG in the frame d-q are given by [12]:

$$\begin{cases} V_{ds} = R_s i_{ds} + \dot{\varphi}_{ds} - \omega_s \varphi_{qs} \\ V_{qs} = R_s i_{qs} + \dot{\varphi}_{qs} + \omega_s \varphi_{ds} \\ V_{dr} = R_r i_{dr} + \dot{\varphi}_{dr} - \omega_r \varphi_{qr} \\ V_{qr} = R_r i_{qr} + \dot{\varphi}_{qr} + \omega_r \varphi_{dr} \end{cases} \quad (12)$$

with: $\omega_r = \omega_s - \omega$

$$\begin{cases} \varphi_{ds} = L_s i_{ds} + M i_{dr} \\ \varphi_{qs} = L_s i_{qs} + M i_{qr} \\ \varphi_{dr} = L_r i_{dr} + M i_{ds} \\ \varphi_{qr} = L_r i_{qr} + M i_{qs} \end{cases} \quad (13)$$

Where R_s, R_r, L_s and L_r are respectively resistances and inductances of the stator and the rotor winding. M is the mutual inductance. V_{ds}, V_{qs}, V_{dr}, V_{qr}, i_{ds}, i_{qs}, i_{dr}, i_{qr}, φ_{ds}, φ_{qs}, φ_{dr} and φ_{qr} are respectively the direct and quadrate components of the stator and the rotor voltages, currents and flux.

The expression of the electromagnetic torque is given by Eq. (14):

$$T_e = p(\varphi_{ds} i_{qs} - \varphi_{qs} i_{ds}) \quad (14)$$

4. Topologies and Controls of the DFIG

4.1. Back to back converter

Figure 3 shows the architecture of the system where the stator is directly connected to the grid and the rotor is connected to the grid through the back to back converter. The converter contains two parts, the first one connected to the machine called rotor side converter "RSC" and the second one connected to the network called grid side converter "GSC". This means, two loops control exist, one for the RSC converter, which control the statorique active and reactive powers, and one for the GSC converter, which regulate the DC bus voltage between the RSC and the GSC and adjust the power factor on the network side.

Concerning the principle control of RSC (shown in Fig.4), we notice that the fluxes and currents are strongly coupled (see Eq. (14)) which is necessary to use the vector control where the d-q reference frame is linked to the rotating field. By orienting the stator flux along the axis d we obtain equation (15). In this study the frequency and the voltage are considered constant.

$$\begin{cases} \varphi_{ds} = \varphi_s \\ \varphi_{qs} = 0 \end{cases} \quad (15)$$

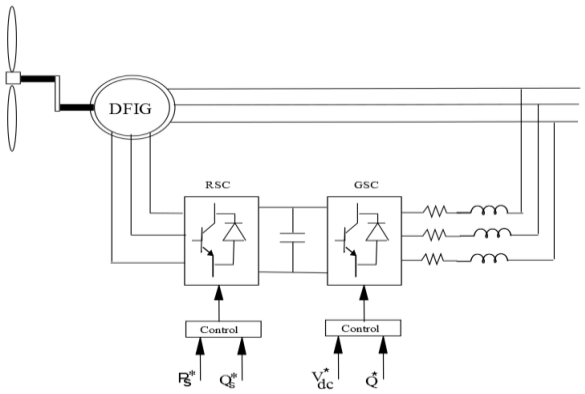

Fig. 3. System control architecture with back to back converter

Moreover, the stator current can be written as follow:

$$\begin{cases} I_{ds} = \dfrac{\varphi_{ds} - M I_{dr}}{L_s} \\ I_{qs} = \dfrac{-M I_{qr}}{L_s} \end{cases} \quad (16)$$

And the electromagnetic torque is expressed as follows:

$$T_{em} = -\frac{pM}{L_s} \varphi_s i_{qr} \quad (17)$$

Usually, the power of the machines used in wind energy production is medium or high, which means that the stator resistance is neglected. Assuming that the stator flux is constant, the stator voltage becomes:

$$\begin{cases} V_{ds} = 0 \\ V_{qs} = V_s = \omega_s \varphi_{ds} \end{cases} \quad (18)$$

Moreover, the active and reactive powers in the stator and the rotor are respectively defined as [11]:

The stator:

$$\begin{cases} P_s = V_{ds} i_{ds} + V_{qs} i_{qs} \\ Q_s = V_{qs} i_{ds} - V_{ds} i_{qs} \end{cases} \quad (19)$$

The rotor:

$$\begin{cases} P_r = V_{dr} i_{dr} + V_{qr} i_{qr} \\ Q_r = V_{qr} i_{dr} - V_{dr} i_{qr} \end{cases} \quad (20)$$

From the equations (16)-(18)-(19) and (20) the power expressions are deduced:

$$\begin{cases} P_s = -V_s \dfrac{M}{L_s} I_{qr} \\ Q_s = \dfrac{V_s \varphi_s}{L_s} - \dfrac{V_s M}{L_s} I_{dr} \end{cases} \quad (21)$$

and

$$\begin{cases} P_r = s V_s \dfrac{M}{L_s} I_{qr} \\ Q_r = s \dfrac{V_s M}{L_s} I_{dr} \end{cases} \quad (22)$$

The total active and reactive powers of the wind generator are given by:

$$\begin{cases} P_t = P_s + P_r = (s-1) V_s \dfrac{M}{L_s} I_{qr} \\ Q_t = Q_s + Q_r = \dfrac{V_s \varphi_s}{L_s} - (s-1) \dfrac{V_s M}{L_s} I_{dr} \end{cases} \quad (23)$$

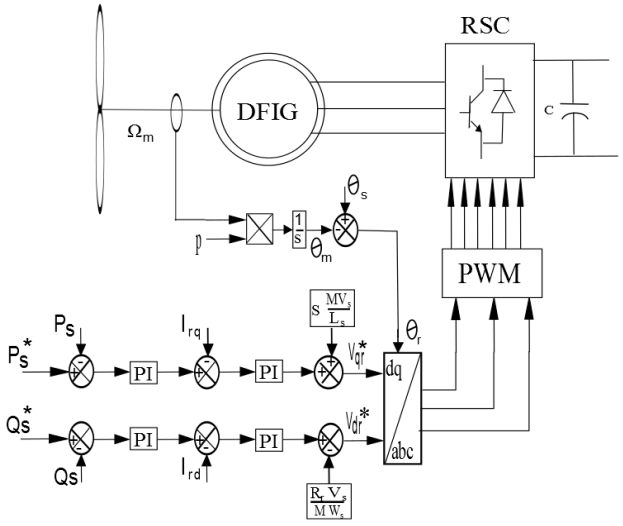

Fig. 4. Control principle of rotor side converter

In the other side, for the principle control of GSC (shown in Fig.5), a first order filter (RL) is connected between the GSC and the network. By applying Kirchhoff law we obtain the following Equation:

$$[V_{mk}] = R_t [i_k] + L_t [i_k] + [V_{pk}] \quad (24)$$

where: k=1, 2, 3.

In the d-q reference frame the equation (24) can be written as:

$$\begin{cases} V_{md} = R_t i_d + L_t \dfrac{d}{dt} i_d - L_t \omega_s i_q + V_{pd} \\ V_{mq} = R_t i_q + L_t \dfrac{d}{dt} i_q + L_t \omega_s i_d + V_{pq} \end{cases} \quad (25)$$

We suppose that:

$$\begin{cases} V_{td} = R_t i_d + L_t \dfrac{d}{dt} i_d \\ V_{tq} = R_t i_q + L_t \dfrac{d}{dt} i_q \end{cases} \quad (26)$$

Then from Eq. (25) and Eq. (26) we obtain:

$$\begin{cases} V_{td} = V_{md} + L_t \omega_s i_q - V_{pd} \\ V_{tq} = V_{md} - L_t \omega_s i_q - V_{pd} \end{cases} \quad (27)$$

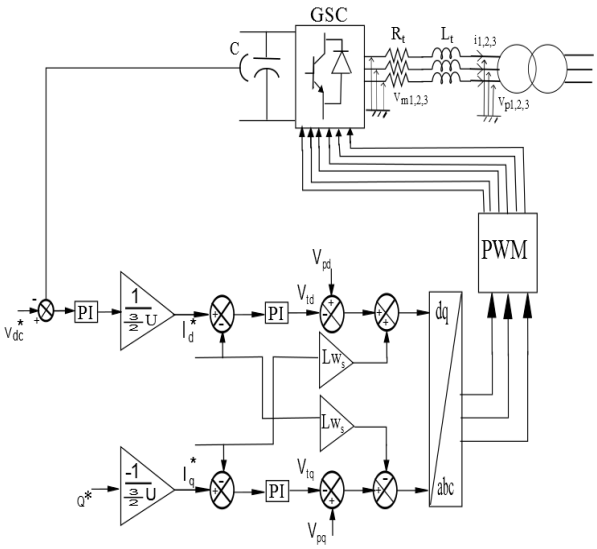

Fig. 5. Control principle of grid side converter

The converters are bidirectional, the RSC and GSC work as rectifier and inverter respectively when the slip is negative (super-synchronous mode) and when the slip is positive (sub-synchronous mode) the RSC and GSC work as inverter and rectifier respectively. The simulation results of this topology are given by the Fig.6 to Fig.9. Fig.6 and Fig.7 show the active and reactive powers of the stator where the reference given to the powers are $P_s^* = -\eta . P_m$ and $Q_s^* = 0$ for a unit power factor, Fig.8 and Fig.9 give the generated current and its FFT where the THD obtained is 22.47%.

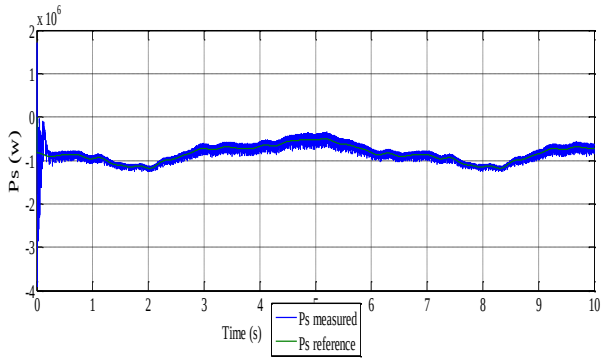

Fig. 6. Stator active power

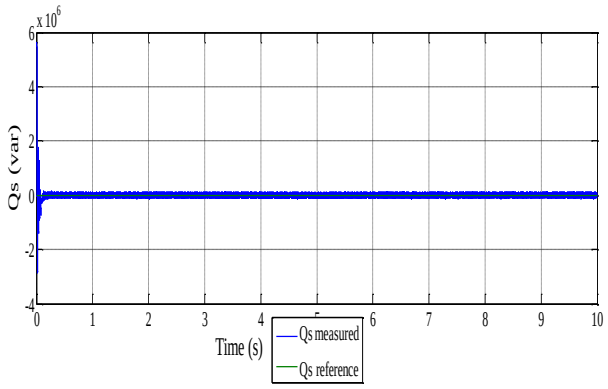

Fig. 7. Stator reactive power

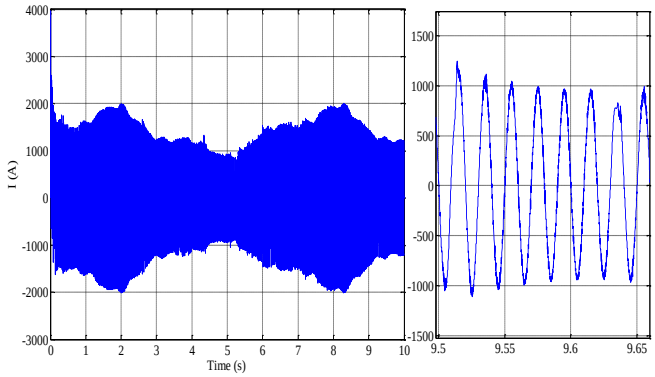

Fig. 8. Generated current

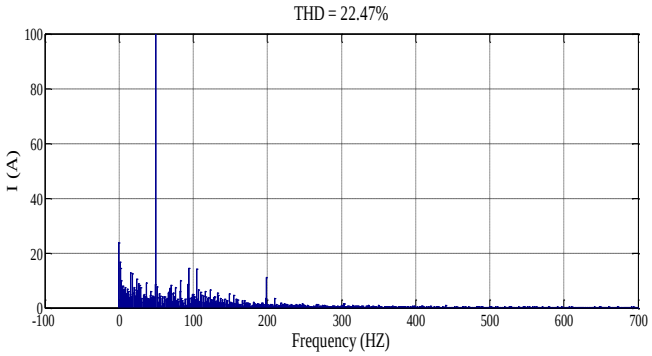

Fig. 9. FFT analysis

4.2. Matrix converter

The system is illustrated on the Fig.10, as in the previous structure the stator is directly connected to the network; the rotor is connected to the grid through the matrix converter.

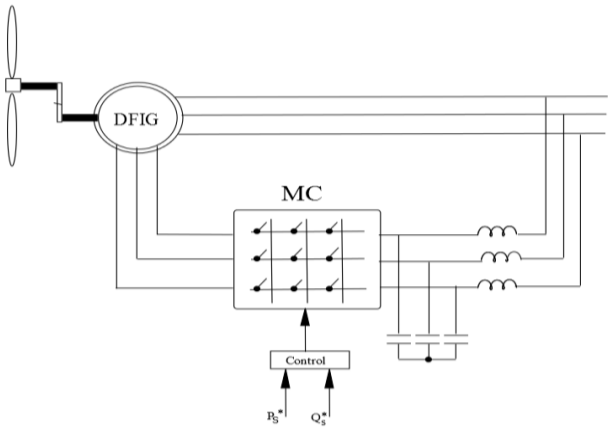

Fig. 10. System control architecture with matrix converter

Counter to the previous structure this one needs only one control loop where the stator powers are controlled; the power factor is regulated through the matrix converter and the transfer of energy is direct without using any element of storage.

The matrix converter is an AC-AC converter, which is composed by 9 bi-directional switches. Further, it's a structure that provides sinusoidal output with a desirable frequency and amplitude. Figure 11 shows the three-phase matrix converter:

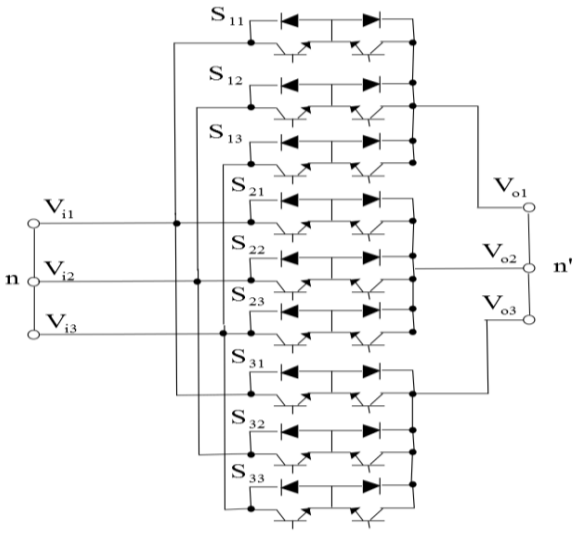

Fig. 11. Basic three phase matrix converter

The S_{jk} represents the bidirectional switches; V_i and V_o are the input and output voltages respectively. The relationship between the output and input voltages is given as [13]:

$$\begin{bmatrix} v_{o1n'} \\ v_{o2n'} \\ v_{o3n'} \end{bmatrix} = \begin{bmatrix} m_{11} & m_{12} & m_{13} \\ m_{21} & m_{22} & m_{23} \\ m_{31} & m_{32} & m_{33} \end{bmatrix} \begin{bmatrix} v_{i1n} \\ v_{i2n} \\ v_{i3n} \end{bmatrix} \quad (28)$$

m_{jk} are the coefficients of modulation. The sum of the coefficients of modulation used to synthesize the same output phase must be equal to 1.

V_i and V_o are defined as:

$$\begin{bmatrix} v_{i1n} \\ v_{i2n} \\ v_{i3n} \end{bmatrix} = V_i \begin{bmatrix} \cos(\omega_i t) \\ \cos(\omega_i t + 2\pi/3) \\ \cos(\omega_i t - 2\pi/3) \end{bmatrix} \quad (29)$$

$$\begin{bmatrix} v_{o1n'} \\ v_{o2n'} \\ v_{o3n'} \end{bmatrix} = q \times V_i \begin{bmatrix} \cos(\omega_o t) \\ \cos(\omega_o t + 2\pi/3) \\ \cos(\omega_o t - 2\pi/3) \end{bmatrix} + v_{nn'} \quad (30)$$

$q = V_o / V_i = [0, 0.866]$: represents the voltage ratio.

The control of matrix converter consists of two steps as shown on Fig.12. In the first one, the coefficients of modulation m_{jk} are calculated through the control algorithm. Then the m_{jk} elements are transformed to coefficients of connection c_{jk} through a PWM to control the switches.

In this study, the control strategy used to calculate the m_{jk} elements is Ph D method [9].

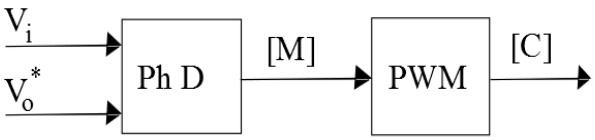

Fig. 12. Matrix converter modulation steps

The elements m_{jk} of the matrix [M] are given by the following equations [9]:

$$m_{jk} = a_j + \frac{v_{jn}(v_{kn'} - v_{nn'})}{v^2_{i1n} + v^2_{i2n} + v^2_{i3n}} \quad (31)$$

with j=1,2,3 ; k=1,2,3.

a_j and $v_{nn'}$ are defined as:

$$v_{nn'} = \frac{Max(v_{i1n}, v_{i2n}, v_{i3n}) + Min(v_{i1n}, v_{i2n}, v_{i3n})}{2} \quad (32)$$

$$a_j = \frac{|v_{jn}| - \frac{|v_{i1n}| + |v_{i2n}| + |v_{i3n}|}{3}}{2\sqrt{\frac{2}{3}(v^2_{i1n} + v^2_{i2n} + v^2_{i3n})}} + 1/3 \quad (33)$$

The c_{jk} are obtained from the m_{jk} by using a PWM. Where c_{11}, c_{21}, c_{31} are deducted by comparing m_{11}, m_{21}, m_{31} to a saw tooth seated right, by proceeding with the same way and using a saw tooth seated left the c_{12}, c_{22}, c_{32} are obtained from m_{12}, m_{22}, m_{32}, finally the c_{13}, c_{23}, c_{33} are complementary to 1 (Eq. (34)), an example of the PWM is given on [9]:

$$\begin{cases} c_{11} + c_{12} + c_{13} = 1 \\ c_{21} + c_{22} + c_{23} = 1 \\ c_{31} + c_{32} + c_{33} = 1 \end{cases} \quad (34)$$

The simulations results of this topology are given by the following schemes, Fig.13 and 14 show the active and the reactive powers of the stator, Fig.15 shows the generated current, and the FFT of the current in Fig.16 gives a THD=19.00%.

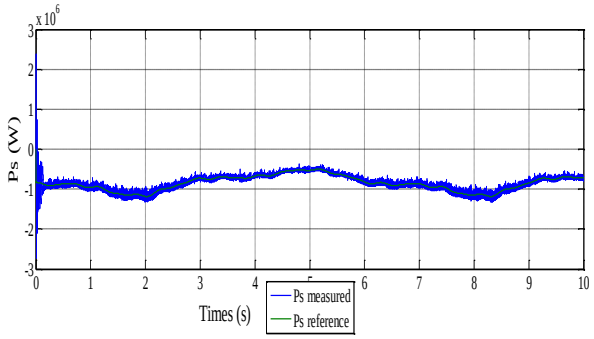

Fig. 13. Stator active power

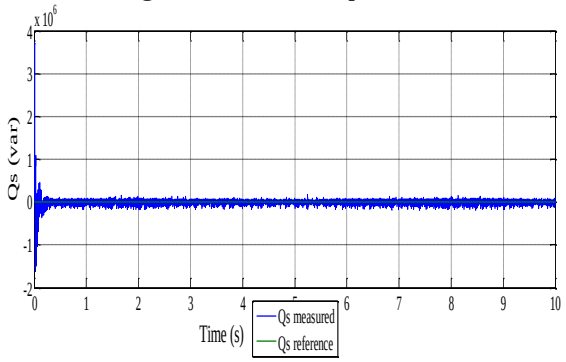

Fig. 14. Stator reactive power

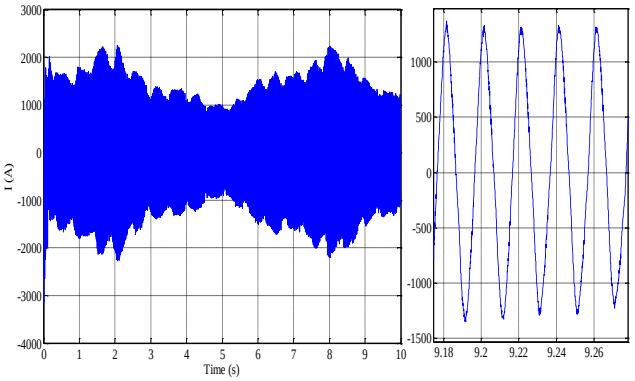

Fig. 15. Generated current

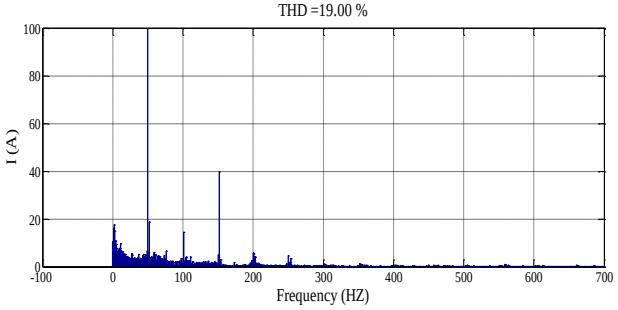

Fig. 16. FFT analysis

5. Power Losses Calculation

This part investigates the loss of power in both topologies. There are two kinds of losses, the conduction and the switching losses. This study includes the evolution of total losses according to rotation speed of the DFIG.

The converters consist of bi-directional switches and each one is composed by semiconductors (IGBT and Diode).

The calculation of total losses is speared on conduction and switching losses for each semiconductor, the conduction losses for the IGBTs and Diodes are given by [14]:

$$P_{cond,IGBT}(t) = V_{ce0} I(t) + r_{ce} I^2(t) \quad (35)$$

V_{ce0} , r_{ce} and I represent the collector-emitter voltage at zero current, the equivalent on-resistance and the rms magnitude current respectively. Where the V_{ce0} , r_{ce} are determined from the data-sheet of the constructor.

$$P_{cond,DIODE}(t) = V_{f0} I(t) + r_d I^2(t) \quad (36)$$

V_{f0} and r_d represent the diode forward voltage drop at zero current and the equivalent on-resistance for the diode.

Matrix converter consists of 18 IGBTs and 18 Diodes and the back to back converter consists of 12 IGBTs and 12 Diodes. However the output current in matrix converter flows through an IGBT and a diode at all-time, the total conduction losses per phase in matrix converter can expressed as [14]:

$$P_{cond,phase}(t) = (V_{ce0} + V_{f0}).I.\frac{2\sqrt{2}}{\pi} + (r_{ce} + r_d)I^2 \quad (37)$$

In back to back converter the output current flows through an IGBT or its anti-parallel diode depending on the current direction.

The total switching losses depend on turn-on W_{on} and turn-off W_{off} energy loss for an IGBT Fig.17 and the recovery energy loss W_{rec} for a diode. The switching losses equations are defined as [15]:

$$W_{on} = \frac{1}{2} V_{ce} I.t_{on} \quad (38)$$

With $t_{on} = t_{ri} + t_{fv}$, where t_{ri}, t_{fv} represent the current rise time and the voltage fall time respectively, V_{ce} is the collector-emitter voltage, I is the collector current:

$$W_{off} = \frac{1}{2} V_{ce} I.t_{off} \quad (39)$$

With $t_{off} = t_{rv} + t_{fi}$, where t_{rv}, t_{fi} are the voltage rise time and the current fall time respectively.

$$W_{rec} = V_{ce}.Q_r \quad (40)$$

Where $Q_r = t_r I$ is the reverse recovered charge as shown in Fig.18.

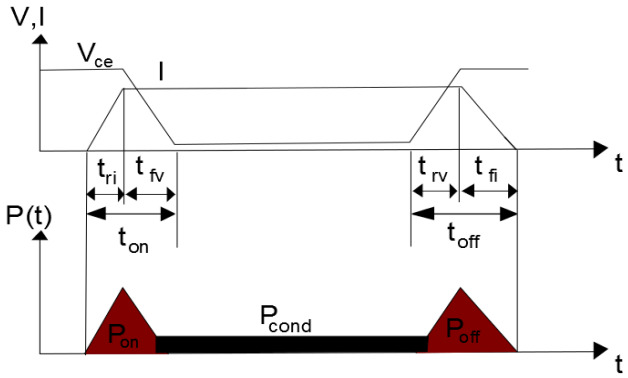

Fig. 17. Instantaneous conduction and switching waveforms of an IGBT

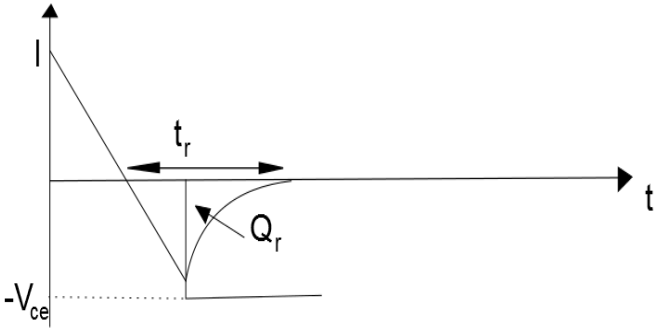

Fig. 18. Switching waveforms of a Diode

The characteristics of IGBTs and Diodes used to calculate the power losses are the same in both converters. The total losses of both converters are given by Fig.19; it shows that the matrix converter is more efficiency than back to back converter. Moreover, when the system operates on the super-synchronous mode the efficient is proportional to the speed, in the other parts (sub-synchronous mode) the efficient decreases when the speed increase.

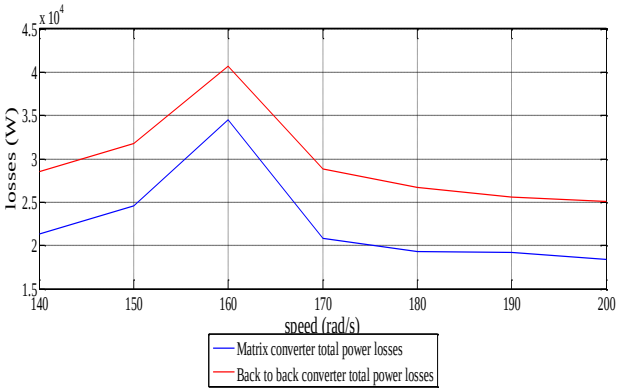

Fig. 19. Power losses in converters

Table 1 summarizes the comparison points. Due to the transformation ratio q, the output voltage of the matrix converter topology is lower than the back to back one. Additionally, the matrix converter requires 18 IGBTs and 18

Diodes while back to back converter requires only 12 IGBTs and 12 Diodes.

Table 1. Comparison points

	Matrix converter topology	Back to back converter topology
Output voltage	593,4 v	690 v
IGBTs	18	12
Diodes	18	12
Loops control	1	2
Input filter	LC	RL
Switching frequency	10 kHz	10 kHz
DC link voltage	-	1200 v
Voltage measurement	6	7
Current measurement	6	9

The whole system based on matrix converter needs one loop control where active and reactive powers on the stator are controlled, this topology uses 6 voltages and current measurements. On the other hand the system based on back to back converter contains: two control loops (one of each stage), 7 voltage and 9 current measurements are needed. This comparison shows that the structure based on the matrix converter is more economical than the structure based on back-to-back converter as it requires fewer sensors.

The input filters are also concerned, the matrix converter uses LC filter which is considered as a low pass filter to eliminate the harmonics. Although the back to back uses a RL filter to remove the anomaly between the capacitor (DC link) and the input source.

Switching frequency has been chosen 10 kHz for matrix converter and back to back converter which is corresponding to 100 μs of a period cycle.

The energy transfer in matrix converter is directly counter to back to back converter where a storage element is needed. While it is known that DC capacitor contains losses which can be added to the converter losses. In this work, this part is not considered.

6. Conclusion

This work evaluates the performance of wind turbine system, where the generator (DFIG) is fed by back to back converter which is the most affordable and discussed. We are also interested on feeding the DFIG through a matrix converter which performance is questionable in wind turbine application. Comparing the generated current and the power losses delivered by the same generator, the results show that the topology with a matrix converter has the better performance, we realized that the THD and total power losses of back to back converter topology was higher than the matrix converter topology. From this study we can conclude that it is better to feed the DFIG by a matrix converter.

References

[1] M. Mansour, M.N. Mansouri, M.F. Mmimouni. "Study and Control of a Variable-speed Wind-Energy System Connected to the Grid ". *International Journal of Rewenable Energy Research*. vol 1, pp 96-104, 2011. (Article)

[2] RC Portillo. ;MM Prats, J.I Leon;J.A Sanchez, J.M Carrasco,E Galvan, and LG Franquelo, "Modeling Strategy for Back-to-Back Three-Level Converters Applied to High-Power Wind Turbines". *IEEE Transactions on industrial electronics*, Vol 53. pp.1483-1491, 2006. (Article)

[3] E.J Bueno,.S Cobreces,. F.J Rodriguez, A Hernandez, and F Espinosa. "Design of a Back-to-Back NPC Converter Interface for Wind Turbines With Squirrel-Cage Induction Generator". *IEEE Transactions on Energy conversion*, vol 23 (no.3): p.932-945. 2008. (Article)

[4] R Pena, JC Clare and GM Asher,. "Doubly fed induction generator using back-to-back PWM converters and its application to variable-speed wind-energy generation". *IEE Proceedings-electrical power applications*, vol 143 (no.3): p. 231-241. 2002. (Article)

[5] Lee JH, Jeong JK, Han BM, Choi NS and Cha HJ. "DFIG Wind Power System with a DDPWM Controlled Matrix Converter". *Journal of Electrical Engineering & Technology*, Vol 5, pp. 299-306, 2010.(Article)

[6] K.E. Okedu. "matrix converter control for DFIG". *IEEE International Conference on Emerging & sustainable Technologies for Power & ICT in a Developing Society*. Owerri, pp. 273-277, 14-16 November 2013. (Conference Paper)

[7] R Cárdenas, R Pena, P Wheeler, J Clare,A Munoz and A, Sureda "A. Control of a wind generation system based on a Brushless Doubly-Fed Induction Generator fed by a matrix converter". *Electric Power System Reaserch*, Vol 103, pp 49– 60, 2013.(Article)

[8] L Zhang, C Watthanasarn "A Matrix Converter Excited Double-Fed Induction Machine as a Wind Power Generator" *7th International Conference on Power Electronics and Variable Speed Drives*, London, pp. 532-537, 21-23 September 1998. (Conference Paper).

[9] P Delarue, C Rombaut, G Suegier. *les convertisseurs de l'électronique de puissance la conversion alternatif-alternatif*, 3rd ed. vol 2 ",. TEC&DOC Lavoisier, 2006,pp 325-356.(Book)

[10] H Altun, S Sunter .Modeling, simulation and control of wind turbine driven doubly-fed induction generator with matrix converter on the rotor side. *Electrical*

Eengineering-Springer. Vol 95, pp. 157-170, 2013. (Article).

[11] A.Moualdia, MO Mahoudi, L Nezli, and O Bouchhida."Modelling and Control of Wind Power Conversion System Based on the Double fed Asynchronous generator". *International Journal of Rewenable Energy Research*. vol 2, pp 300-306, 2012. (Article).

[12] A Nazari, H Heydari. "A Survey on Different Direct Power Control Algorithms of DFIGs." *2nd Power Electronics, Drive Systems and Technologies Conference*, Tehran, pp 10-14, 16-17 February 2011. (Conference Paper).

[13] B Metidji,N Taib,L Baghli,T Rekioua, and S Bacha: "Novel Single Current Sensor Topology for Venturini Controlled Direct Matrix Converters" *IEEE Transactions on Power Electronics*. Vol 28, pp. 3509 – 3516, 2013,(Article)

[14] M Apap; JC Clare, PW Wheeler, M Bland and K Bradley. "Comparison of losses in matrix converters and voltage source inverters." *Matrix converters, IEE Seminar*, pp. 4/1-4/6, 1 April 2003. (Conference Paper).

[15] S Lefebvre, F Miserey. *Composants a semi-conducteur pour l'electronique de puissance*.1st ed. Paris, France : TEC&DOC Lavoisier: 2004. (Book)